



**STRENGTH ANALYSIS AND DESIGN OF
MULTILAYERED THICK COMPOSITE
SPHERICAL PRESSURE VESSELS**

Ajit K. Roy
University of Dayton Research Institute
300 College Park Avenue
Dayton, OH 45469-0168

MARCH 1991

Final Report for the Period May 1990 - August 1990

Approved for public release; distribution unlimited.

DTIC
SELECTED
JUN 04 1991
S B D

MATERIALS LABORATORY
WRIGHT LABORATORY
AIR FORCE SYSTEMS COMMAND
WRIGHT-PATTERSON AIR FORCE BASE, OH 45433-6533

91-00903



91 5 30 054

NOTICE

WHEN GOVERNMENT DRAWINGS, SPECIFICATIONS, OR OTHER DATA ARE USED FOR ANY PURPOSE OTHER THAN IN CONNECTION WITH A DEFINITELY GOVERNMENT-RELATED PROCUREMENT, THE UNITED STATES GOVERNMENT INCURS NO RESPONSIBILITY OR ANY OBLIGATION WHATSOEVER. THE FACT THAT THE GOVERNMENT MAY HAVE FORMULATED OR IN ANY WAY SUPPLIED THE SAID DRAWINGS, SPECIFICATIONS, OR OTHER DATA, IS NOT TO BE REGARDED BY IMPLICATION, OR OTHERWISE IN ANY MANNER CONSTRUED, AS LICENSING THE HOLDER, OR ANY OTHER PERSON OR CORPORATION; OR AS CONVEYING ANY RIGHTS OR PERMISSION TO MANUFACTURE, USE, OR SELL ANY PATENTED INVENTION THAT MAY IN ANY WAY BE RELATED THERETO.

THIS REPORT HAS BEEN REVIEWED BY THE OFFICE OF PUBLIC AFFAIRS (ASD/PA) AND IS RELEASABLE TO THE NATIONAL TECHNICAL INFORMATION SERVICE (NTIS). AT NTIS IT WILL BE AVAILABLE TO THE GENERAL PUBLIC INCLUDING FOREIGN NATIONS.

THIS TECHNICAL REPORT HAS BEEN REVIEWED AND IS APPROVED FOR PUBLICATION.

Kenneth M. Johnson

KENNETH M. JOHNSON, Project Engineer
Structural Materials Branch
Nonmetallic Materials Division

Charles E. Browning

CHARLES E. BROWNING, Chief
Structural Materials Branch
Nonmetallic Materials Division

FOR THE COMMANDER

George F. Schmidt Jr.

MERRILL L. MINGES, SES
Director
Nonmetallic Materials Division

IF YOUR ADDRESS HAS CHANGED, IF YOU WISH TO BE REMOVED FROM OUR MAILING LIST, OR IF THE ADDRESSEE IS NO LONGER EMPLOYED BY YOUR ORGANIZATION PLEASE NOTIFY WL/MLBC: WRIGHT-PATTERSON AFB, OH 45433-6533 TO HELP MAINTAIN A CURRENT MAILING LIST.

COPIES OF THIS REPORT SHOULD NOT BE RETURNED UNLESS RETURN IS REQUIRED BY SECURITY CONSIDERATIONS, CONTRACTUAL OBLIGATIONS, OR NOTICE ON A SPECIFIC DOCUMENT.

REPORT DOCUMENTATION PAGE

Form Approved
OMB No. 0704-0188

Public reporting burden for this collection of information is estimated to average 1 hour per response, including the time for reviewing instructions, searching existing data sources, gathering and maintaining the data needed, and completing and reviewing the collection of information. Send comments regarding this burden estimate or any other aspect of this collection of information, including suggestions for reducing this burden, to Washington Headquarters Services, Directorate for Information Operations and Reports, 1215 Jefferson Davis Highway, Suite 1204, Arlington, VA 22202-4302, and to the Office of Management and Budget, Paperwork Reduction Project (0704-0188), Washington, DC 20503.

1. AGENCY USE ONLY (Leave blank)			2. REPORT DATE		3. REPORT TYPE AND DATES COVERED		
			March 1991		Final Report - May-August 1990		
4. TITLE AND SUBTITLE			5. FUNDING NUMBERS				
STRENGTH ANALYSIS AND DESIGN OF MULTILAYERED THICK COMPOSITE SPHERICAL PRESSURE VESSELS			F33615-87-C-5239 Program Element 62102F Project No. 2419 Task No. 02 Work Unit Accession #25				
6. AUTHOR(S)			8. PERFORMING ORGANIZATION REPORT NUMBER				
Ajit K. Roy			UDR-TR-90-128				
7. PERFORMING ORGANIZATION NAME(S) AND ADDRESS(ES)			10. SPONSORING/MONITORING AGENCY REPORT NUMBER				
University of Dayton Research Institute 300 College Park Avenue Dayton, OH 45469-0168			WRDC-TR-90-4141				
9. SPONSORING/MONITORING AGENCY NAME(S) AND ADDRESS(ES)							
Materials Laboratory (WL/MLBC) Wright Laboratory (K. Johnson, 255-9073) Air Force Systems Command Wright-Patterson AFB, OH 45433-6533							
11. SUPPLEMENTARY NOTES							
12a. DISTRIBUTION / AVAILABILITY STATEMENT			12b. DISTRIBUTION CODE				
Approved for public release; distribution unlimited.							
13. ABSTRACT (Maximum 200 words)							
A design study of a multilayered spherical composite pressure vessel is presented. Each layer of the vessel is composed of quasi-isotropic layups of composite plies. For the stress analysis, however, each layer is assumed to be homogeneous whose three-dimensional properties are equivalent to that of the quasi-isotropic plies. The linear theory of elasticity is employed so that the analysis is not limited to any thickness of the vessel. For the strength analysis the Tsai-Wu failure criterion is used. Using the ply constitutive law and lamination angle, the ply stresses and strains are determined from the layer stresses and strains. Then the failure criterion is used for each ply. It is found that the first-ply-failure (FPF) controls the final failure.							
The objective of this study is to design a spherical vessel with an acceptable safety factor to operate at 200 MPa internal pressure. In view of the winding and manufacturing difficulties, a design restriction of $b/a < 1.25$ was set for this design. However a two-layered hybrid sphere of $b/a=1.25$ (b : outer radius, a : inner radius) with T300/5208 and IM6/epoxy outside is considered to be an acceptable design. The failure test data of two vessels are also reported in this study.							
14. SUBJECT TERMS			15. NUMBER OF PAGES				
laminated sphere, graphite/epoxy, thick, design, multilayered, burst pressure, failure pressure			45				
16. PRICE CODE							
17. SECURITY CLASSIFICATION OF REPORT		18. SECURITY CLASSIFICATION OF THIS PAGE		19. SECURITY CLASSIFICATION OF ABSTRACT		20. LIMITATION OF ABSTRACT	
Unclassified		Unclassified		Unclassified		UL	

FOREWORD

The work reported herein was performed at Ecole National Supérieure des Mines de Saint-Etienne (EMSE), France, under a collaborative program between the WL Materials Laboratory and EMSE. This work was performed by Ajit K. Roy of the University of Dayton Research Institute under Contract No. F33615-87-C-5239 for the period from May 1990 to August 1990.

ACKNOWLEDGEMENT

The author wishes to thank Professor Georges Verchery of EMSE and Dr. Thierry Massard of Commissariat à l'Energie Atomique (CEA), France for their technical assistance and encouragement.

Accession For	
NTIS GRA&I	<input checked="" type="checkbox"/>
DTIC TAB	<input type="checkbox"/>
Unannounced	<input type="checkbox"/>
Justification	
By _____	
Distribution/	
Availability Codes	
Dist	Avail and/or Special
A-1	

TABLE OF CONTENTS

SECTION	PAGE
1. INTRODUCTION	1
2. EQUATIONS FOR STRESSES AND STRAINS FOR MULTI-LAYER SPHERE	2
3. STRESSES AND STRAINS FOR SINGLE LAYER SPHERE	5
4. FAILURE CRITERION FOR THREE-DIMENSIONAL LAMINATES	5
5. STRENGTH ANALYSIS OF SPHERES	6
6. BURST AND COLLAPSE PRESSURE OF SPHERES MADE OF ONE MATERIAL	8
7. BURST AND COLLAPSE PRESSURE OF SPHERES MADE OF TWO MATERIALS	9
8. CONCLUSIONS	11
REFERENCES	13
APPENDIX A: Method of Predicting Three-Dimensional Effective Moduli of Laminates	14
APPENDIX B: Instructions for Executing the FORTRAN Program "Sphere"	23

LIST OF ILLUSTRATIONS

FIGURE	PAGE
1. Coordinate system	1
2. Cross section of the sphere and interlayer tractions, q_i , used in the analysis	3
3. 3-D quadratic failure criterion for a transversely isotropic material	6
4. Relations between ply stress and laminate stress in a 3-D thick laminate	7
5. The best-fit interaction term in the isotropic plane based on the measured uniaxial compressive strength	7
6. The burst pressures of two graphite-epoxy composite spheres as functions of the ratios of radii	9
7. Comparison of the predicted burst pressure with the tested data	10
8. The burst pressure of two hybrid spheres as functions of the layer thickness	11
9. Configuration of the laminated ring and its equivalent homogeneous ring subjected to equal hydrostatic pressure on the inner and outer surface	15
10. Configuration of the laminated beam and its equivalent homogeneous beam under end transverse load	16
11. Configuration of the laminated beam and its equivalent homogeneous beam under uniformly distributed load on the top and bottom surface	19

1. Introduction

Fiber reinforced composites have been used for about two decades for improving the burst (due to internal pressure) and collapse pressure (due to external pressure) of spherical pressure vessels [1-3]. Although several reinforcing patterns had been tried in the past, for example radial filament reinforcement [3], the accepted technology for reinforcing spherical vessels has emerged to be the quasi-isotropic lay-ups in the θ - ϕ plane (θ : colatitude, ϕ : azimuth) (Figure 1).

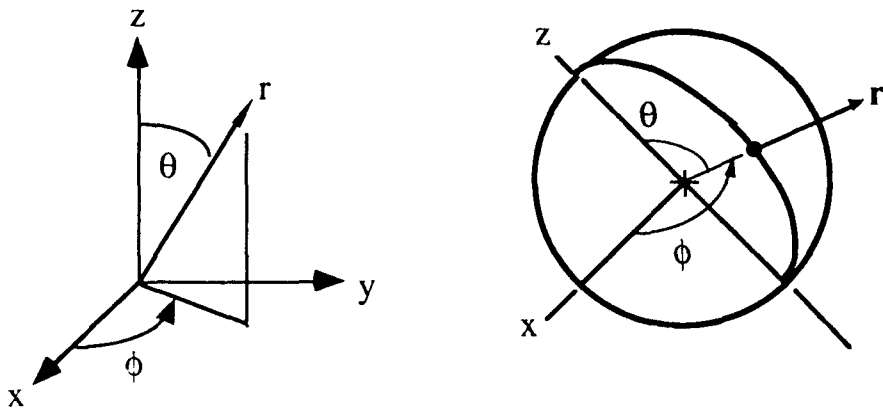


Figure 1. Coordinate System

Gerstle [4] has reported the stress and strength analysis of single-layered fiber reinforced spherical vessels with elastic-ideally plastic bladder. In his work the layer of a vessel is considered to be composed of quasi-isotropic lay-ups of one type of material. Gerstle has found that the burst pressure of a single-layered vessel is limited by the radial compressive strength of the vessel. The radial compressive strength of these vessels, incidentally, is related to the stiffness and transverse compressive strength of the laminae used in the lay-ups. Thus one logical way of improving the failure pressure is to make hybrid vessels where an optimal use of the stiffnesses and strengths of the layers is expected to improve the failure pressure. Gerstle [5] has then presented a similar work for two-layered hybrid spherical vessels and has shown a way to use the stiffnesses and strengths of the two hybrid layers in improving the burst pressure over that of a single-layered vessel. The work presented here is in a way an extension of Gerstle's work and is applicable to any number of layers.

2. Equations for Stresses and Strains for Multilayer Spheres

The effective properties of the layers of a spherical vessel with quasi-isotropic lay-ups are transversely isotropic with isotropy in the the $\theta-\phi$ plane (Figure 1). The vessel is considered spherically symmetric. The stress-strain relations of the i -th layer of the vessel reduce to [6]

$$\sigma_r^{(i)} = C_{rr}^{(i)} \varepsilon_r^{(i)} + 2C_{r\theta}^{(i)} \varepsilon_\theta^{(i)} \quad (1)$$

$$\sigma_\theta^{(i)} = C_{r\theta}^{(i)} \varepsilon_r^{(i)} + (C_{\theta\theta}^{(i)} + C_{\theta\phi}^{(i)}) \varepsilon_\theta^{(i)} \quad (2)$$

$$\varepsilon_r^{(i)} = S_{rr}^{(i)} \sigma_r^{(i)} + 2S_{r\theta}^{(i)} \sigma_\theta^{(i)} \quad (3)$$

$$\varepsilon_\theta^{(i)} = S_{r\theta}^{(i)} \sigma_r^{(i)} + (S_{\theta\theta}^{(i)} + S_{\theta\phi}^{(i)}) \sigma_\theta^{(i)} \quad (4)$$

$$\varepsilon_r^{(i)} = \frac{du_r^{(i)}}{dr}; \quad \varepsilon_\theta^{(i)} = \frac{u_r^{(i)}}{r}; \quad \varepsilon_\phi^{(i)} = \varepsilon_\theta^{(i)} \quad (5)$$

Here $C_{ij}^{(i)}$, $S_{ij}^{(i)}$, ($i, j = r, \theta, \phi$) are the elements of the three-dimensional effective stiffness and compliance matrices of the i -th layer respectively. A method of determining the three-dimensional effective stiffnesses and compliances of a laminate is given in reference [7] and is summarized in Appendix A. If the sphere is subjected to both internal and external pressure, then the boundary conditions are

$$\text{when } r = a \quad \sigma_r^{(1)} = -p \text{ (the negative sign is because of the compressive pressure)} \quad (6)$$

$$\text{when } r = b \quad \sigma_r^{(n)} = -q \text{ (the negative sign is because of the compressive pressure)} \quad (7)$$

At the interface between two adjacent layers the following conditions must be satisfied

$$\text{at the interface } r = a_i \quad \sigma_r^{(i)} = \sigma_r^{(i+1)} \quad (8)$$

$$u_r^{(i)} = u_r^{(i+1)} \quad (9)$$

If we express the stresses, strains, and displacement in terms of the interlayer normal tractions, q_i , (Figure 2)

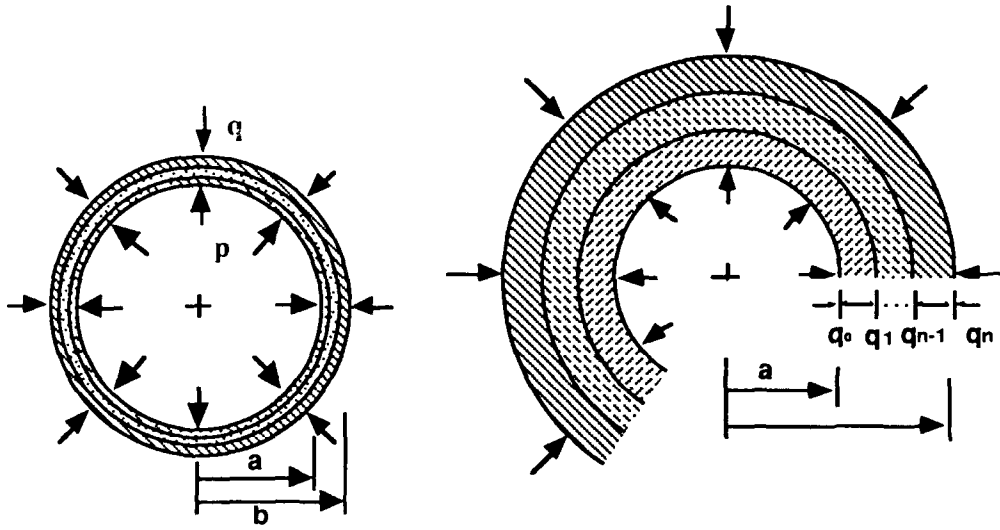


Figure 2. Cross section of the sphere and interlayer tractions, q_i , used in the analysis.

then the expressions for stresses, strains, and displacement of the sphere are:

$$\sigma_r^{(i)} = \frac{1}{1-c_i^{2n_i}} \left[(q_{i-1} c_i^{n_i+\frac{3}{2}} - q_i) \left(\frac{r}{a_i} \right)^{n_i-\frac{1}{2}} - (q_{i-1} - q_i c_i^{n_i-\frac{3}{2}}) c_i^{n_i+\frac{3}{2}} \left(\frac{a_i}{r} \right)^{n_i+\frac{3}{2}} \right] \quad (10)$$

$$\begin{aligned} \sigma_\theta^{(i)} &= \frac{1}{1-c_i^{2n_i}} \left[\frac{C_{\theta\theta}^{(i)} + C_{\theta\phi}^{(i)} + (n_i - \frac{1}{2}) C_{r\theta}^{(i)}}{(n_i - \frac{1}{2}) C_{rr}^{(i)} + 2C_{r\theta}^{(i)}} (q_{i-1} c_i^{n_i+\frac{3}{2}} - q_i) \left(\frac{r}{a_i} \right)^{n_i-\frac{3}{2}} \right] \\ &\quad + \frac{1}{1-c_i^{2n_i}} \left[\frac{C_{\theta\theta}^{(i)} + C_{\theta\phi}^{(i)} - (n_i + \frac{1}{2}) C_{r\theta}^{(i)}}{(n_i + \frac{1}{2}) C_{rr}^{(i)} - 2C_{r\theta}^{(i)}} c_i^{n_i+\frac{3}{2}} (q_{i-1} - q_i c_i^{n_i-\frac{3}{2}}) \left(\frac{a_i}{r} \right)^{n_i+\frac{3}{2}} \right] \end{aligned} \quad (11)$$

$$\sigma_\phi^{(i)} = \sigma_\theta^{(i)} \quad (12)$$

$$\epsilon_r^{(i)} = \frac{1}{1-c_i^{2n_i}} \left[\frac{\left(n_i - \frac{1}{2} \right) (q_{i-1} c_i^{n_i+\frac{3}{2}} - q_i)}{\left(n_i - \frac{1}{2} \right) C_{rr}^{(i)} + 2C_{r\theta}^{(i)}} \left(\frac{r}{a_i} \right)^{n_i-\frac{3}{2}} - \frac{\left(n_i + \frac{1}{2} \right) (q_{i-1} - q_i c_i^{n_i-\frac{3}{2}})}{\left(n_i + \frac{1}{2} \right) C_{rr}^{(i)} - 2C_{r\theta}^{(i)}} c_i^{n_i+\frac{3}{2}} \left(\frac{a_i}{r} \right)^{n_i+\frac{3}{2}} \right] \quad (13)$$

$$\epsilon_\theta^{(i)} = \frac{1}{1-c_i^{2n_i}} \left[\frac{q_{i-1} c_i^{n_i+\frac{3}{2}} - q_i}{\left(n_i - \frac{1}{2} \right) C_{rr}^{(i)} + 2C_{r\theta}^{(i)}} \left(\frac{r}{a_i} \right)^{n_i-\frac{3}{2}} + \frac{q_{i-1} - q_i c_i^{n_i-\frac{3}{2}}}{\left(n_i + \frac{1}{2} \right) C_{rr}^{(i)} - 2C_{r\theta}^{(i)}} c_i^{n_i+\frac{3}{2}} \left(\frac{a_i}{r} \right)^{n_i+\frac{3}{2}} \right] \quad (14)$$

$$\varepsilon_{\phi}^{(i)} = \varepsilon_{\theta}^{(i)} \quad (15)$$

$$u_r^{(i)} = \frac{a_i}{1-c_i^{2n_i}} \left[\frac{q_{i-1} c_i^{n_i+\frac{3}{2}} - q_i}{\left(n_i - \frac{1}{2}\right) C_{rr}^{(i)} + 2C_{r\theta}^{(i)}} \left(\frac{r}{a_i}\right)^{n_i-\frac{1}{2}} + \frac{q_{i-1} - q_i c_i^{n_i-\frac{3}{2}}}{\left(n_i + \frac{1}{2}\right) C_{rr}^{(i)} - 2C_{r\theta}^{(i)}} c_i^{n_i+\frac{3}{2}} \left(\frac{a_i}{r}\right)^{n_i+\frac{1}{2}} \right] \quad (16)$$

where

$$c_i = \frac{a_{i-1}}{a_i}, \quad n_i = \frac{1}{2} \sqrt{1 + 8 \frac{C_{\theta\theta}^{(i)} + C_{\theta\phi}^{(i)} - C_{r\theta}^{(i)}}{C_{rr}^{(i)}}}$$

Incidentally, when $r = a$ equation (10) becomes

$$\sigma_r^{(1)} (r = a_o = a) = -q_o = -p \text{ (inside pressure)} \quad (17)$$

and when $r = b$ equation (10) again reduces to

$$\sigma_r^{(n)} (r = a_n = b) = -q_n = -q \text{ (outside pressure)} \quad (18)$$

By expressing the stresses in terms of the interlayer normal tractions, q_i , equation (8) is automatically satisfied. Then substituting equation (16) into equation (9) we get a set of linear equations to determine the interlayer normal tractions, q_i :

$$\frac{q_{i+1} \alpha_{i+1} a_{i+1}}{c_{i+1}} + q_i (\beta_{i+1} - \beta_i - \gamma_{i+1} - \gamma_i) a_i + q_{i-1} \alpha_i a_{i-1} = 0 \quad (19)$$

$$i = 1, 2, \dots, (n-1)$$

here, $q_o = p$ (internal pressure), $q_n = q$ (external pressure) are known, and

$$\alpha_i = \frac{2n_i C_{rr}^{(i)} c_i^{n_i+\frac{1}{2}}}{\mu_i}$$

$$\beta_i = \frac{\left(1 - c_i^{2n_i}\right) \left(\frac{1}{2} C_{rr}^{(i)} - 2C_{r\theta}^{(i)}\right)}{\mu_i}$$

$$\gamma_i = \frac{n_i \left(1 + c_i^{2n_i}\right) C_{rr}^{(i)}}{\mu_i}$$

$$\mu_i = \left(1 - c_i^{2n_i}\right) \left\{ \left(n_i + \frac{1}{2}\right) C_{rr}^{(i)} - 2C_{r\theta}^{(i)} \right\} \left\{ \left(n_i - \frac{1}{2}\right) C_{rr}^{(i)} + 2C_{r\theta}^{(i)} \right\}$$

The interlayer normal tractions, ($q_i, i = 1, \dots, n-1$), are known by solving equation (19). Then substituting the values of q_i in equations (10-16), the stresses, strains, and displacement for all layers are determined.

3. Stresses and Strains for Single Layer Spheres

If there is only one material for the spherical shell, super and subscripts in the equations above assume only one value; i.e., $i = 1$; then in the inside radius, $r = a_0 = a$; and on the outside radius, $r = a_1 = b$. We can define the ratios of the radii as:

$$c_1 = c = \frac{a_0}{a_1} = \frac{a}{b}$$

All equations in the previous section are simplified for the case of one layer of material which can also represent a homogenized laminated shell.

4. Failure Criterion for Three-Dimensional Laminates

Failure criteria for a three-dimensional body can be easily written down in terms of the most general quadratic form. There will be a maximum of 15 strength parameters.

A transversely isotropic material is a reasonable representation of a unidirectional composite ply if the diameter of the fiber is small relative to the thickness of the ply and there are many fibers randomly distributed in the ply. With this symmetry, the number of strength parameters can be reduced to eight. If we can further invoke the identity between tension-compression stresses and pure shear oriented 45-degrees from the former stresses, this additional relation further reduces the strength parameters in a 3-D transversely isotropic materials to seven.

- $F_{ij}\sigma_i\sigma_j + F_i\sigma_i = 1$, for 3-D contracted notation: $\sigma_q = \sigma_{yz}$, $\sigma_r = \sigma_{zx}$, $\sigma_s = \sigma_{xy}$

$$F_{xx}\sigma_x^2 + F_{yy}\sigma_y^2 + F_{zz}\sigma_z^2 + F_{qq}\sigma_q^2 + F_{rr}\sigma_r^2 + F_{ss}\sigma_s^2$$

$$+ 2F_{xy}\sigma_x\sigma_y + 2F_{xz}\sigma_x\sigma_z + 2F_{yz}\sigma_y\sigma_z + F_x\sigma_x + F_y\sigma_y + F_z\sigma_z + F_q\sigma_q + F_r\sigma_r + F_s\sigma_s = 1$$

No. parameters ↓

15

↓

8

↓

7

- From symmetry: $F_{yy} = F_{zz}$, $F_{rr} = F_{ss}$, $F_{xy} = F_{xz}$, $F_y = F_z$, $F_q = F_r = F_s = 0$

$$F_{xx}\sigma_x^2 + F_{yy}(\sigma_y^2 + \sigma_z^2) + F_{qq}\sigma_q^2 + F_{ss}(\sigma_r^2 + \sigma_s^2)$$

$$+ 2F_{xy}\sigma_x(\sigma_y + \sigma_z) + 2F_{yz}\sigma_y\sigma_z + F_x\sigma_x + F_y(\sigma_y + \sigma_z) = 1$$

- From transverse isotropy: $\sigma_y = -\sigma_z = Q$, other $\sigma_i = 0$

$$F_{yy}(2Q^2) - 2F_{yz}Q^2 = 1, \text{ or } Q^2 = \frac{1}{2(F_{yy} - F_{yz})}, \text{ or } Q = \frac{\sqrt{YY^*}}{\sqrt{2(1 - F_{yz}^*)}}$$

$$\text{where } F_{yz} = F_{yz}^* \sqrt{F_{yy}F_{zz}} = F_{yz}^* F_{yy}, F_{yz}^* = F_{yz}/F_{yy}$$

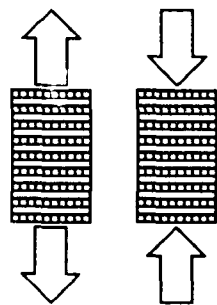
Figure 3. 3-D quadratic failure criterion for a transversely isotropic material

Thus the difference between 2- and 3-D quadratic failure criteria for a unidirectional ply is by only one additional strength parameter. The reduction in the number of strength parameters from 15 to seven is illustrated in Figure 3.

5. Strength Analysis of Spheres

Stress analysis of a spherical shell in 3-D is similar to that for 2-D provided appropriate elastic moduli and stress-strain relations are used. 3-D analysis will of course require 3-D moduli and 3-D stress-strain relations. This is illustrated in Figure 4 where over bars represent the average stress or strain of the 3-D thick laminate. The relation between laminate stress and ply stress is determined with the knowledge of the laminate compliance and ply stiffness, both in 3-D.

$$\{\bar{\epsilon}\} = [\bar{S}]\{\bar{\sigma}\}, \text{ where } [\bar{S}] \text{ is the 3-D laminate compliance}$$



$$\{\sigma\} = [C]\{\bar{\epsilon}\}, \text{ where } [C] \text{ is the 3-D ply stiffness}$$

$$[F_{ij}\sigma_i\sigma_j]R^2 + [F_i\sigma_i]R - 1 = 0,$$

where F_{ij} , F_i are 3-D strength parameters

Assuming unidirectional plies are transversely isotropic:

$$F_{xx}\sigma_x^2 + F_{yy}(\sigma_y^2 + 2F_{yz}^* \sigma_y \sigma_z + \sigma_z^2 + 3\sigma_q^2) + 2F_{xy}\sigma_x(\sigma_y + \sigma_z)$$

$$+ F_{ss}(\sigma_s^2 + \sigma_r^2) + F_x\sigma_x + F_y(\sigma_y + \sigma_z) = 1$$

Figure 4. Relations between ply stress and laminate stress in a 3-D thick laminate. The quadratic failure in 3-D can be applied on a ply-by-ply basis.

In particular, the uniaxial tensile or compressive stress applied along the z-axis can be easily calculated, and the resulting failure strength can also be calculated using the quadratic criterion. The interaction term in the isotropic plane F_{yz}^* can be shown to have a strong influence on the uniaxial compressive strength. The back-calculated interaction term for a typical graphite-epoxy composite is approximately -0.84. This back-calculation is shown in Figure 5 for both thick cross-ply and $[\pm 45]$ laminates.

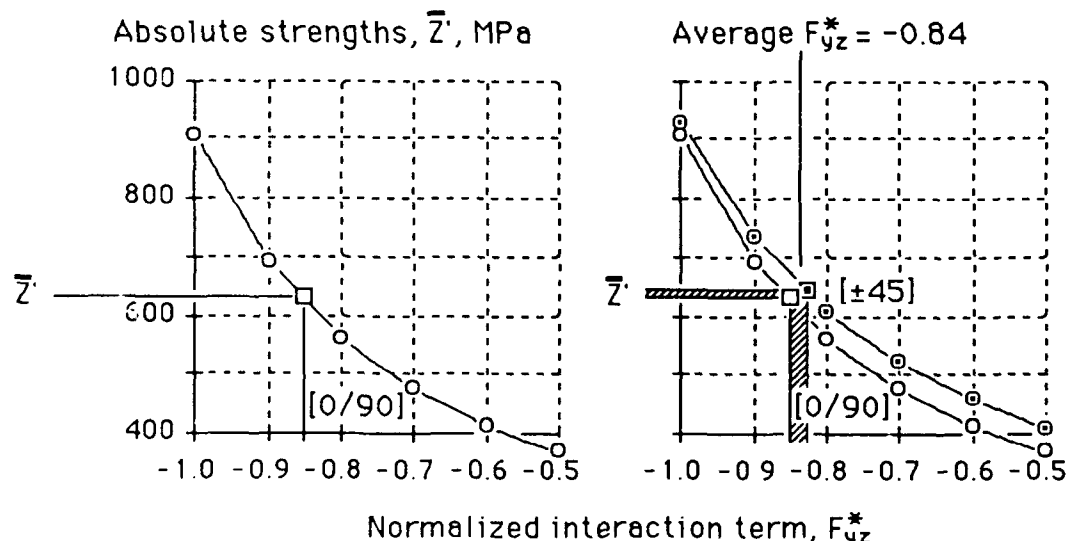


Figure 5. The best-fit interaction term in the isotropic plane based on the measured uniaxial compressive strength.

It is seen that the quadratic failure criterion required a highly coupled relation. The maximum stress or maximum strain criterion assumed that interaction between failure modes does not exist. Based on the test results shown in Figure 5, the predicted maximum compressive strength would be the same as the transverse compressive strength in a unidirectional ply. The value for most graphite-epoxy composites would be in the range of 200 MPa. Thus an error of 300 percent is the result of ignoring failure mode interactions. We therefore believe that the quadratic criterion is flexible in taking into account such mode interactions; while the maximum stress or maximum strain criterion is rigidly defined and does not recognize the interactions.

6. Burst and Collapse Pressure of Spheres Made of One Material

The burst and collapse pressures of a thick spherical shell under internal and external pressures based on strength can be derived using the stress analysis for thick shells coupled with appropriate failure criteria. In the present study, it is assumed that the shell failure is controlled by strength, not by buckling. It is further assumed that the shell consists of homogeneous, quasi-isotropic material with 3-D elastic constants listed in Appendix A.

The predicted burst pressures for typical composite materials are shown in Figure 6. From the equations of stress and strain, it is observed that they are dependent on the ratio of the outside to inside radii, not on their absolute values. The displacements on the other hand are functions of the absolute radii.

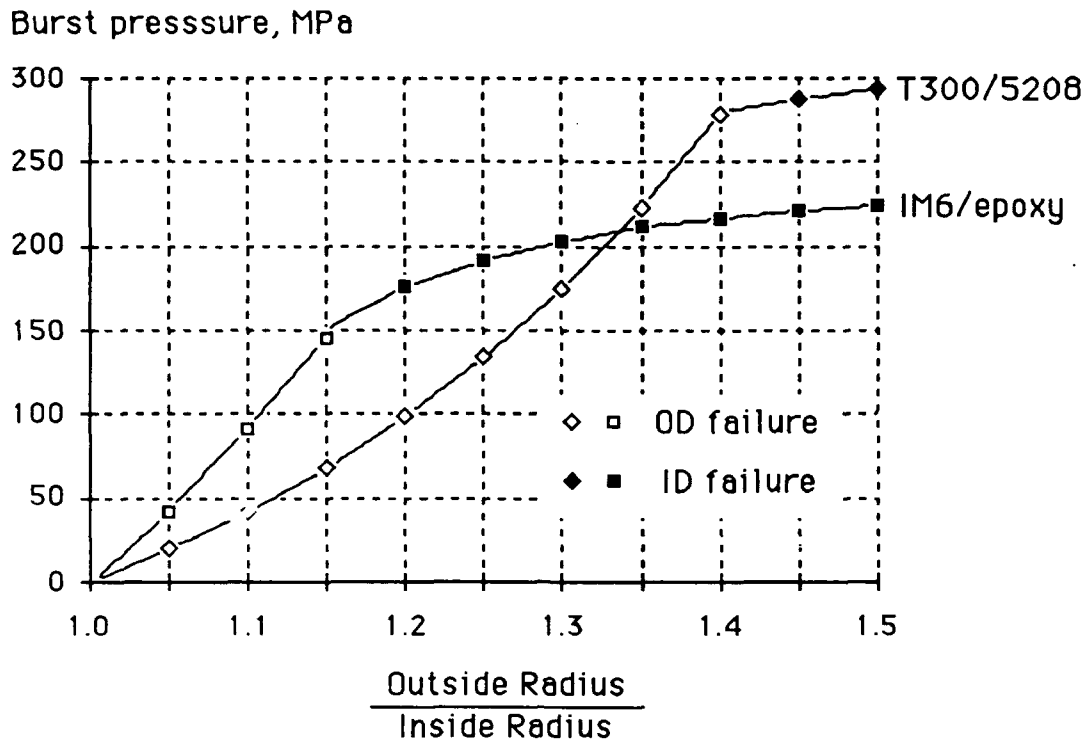


Figure 6. The burst pressures of two graphite-epoxy composite spheres as functions of the ratios of radii.

Open symbols for each material are shown for failure on the outside diameter and solid symbols on the inside. For thin shells failure occurs on the outside; for thick shells failure occurs on the inside. Both materials reach some asymptotic strength level, but their functional dependences on the ratio of radii are different. Below a ratio of 1.35, IM6 has higher burst pressure; above this ratio, T300 becomes higher. It is therefore not possible to guess what material would be stronger unless a calculation is made first.

7. Burst Pressure of Hybrid Spheres Made of Two Materials

One of the objectives of this work is to design a composite sphere to operate at 200 MPa. For the initial design a safety factor of 1.5 was considered. Thus the design of a sphere that could withstand a maximum pressure of 300 MPa was considered to be a safe design. It was initially inferred from Figure 6 that a sphere made with T300/5208 composite of $b/a=1.5$ could take the pressure close to 300 MPa. As a part of a demonstration of the design, a T300/epoxy sphere of inner diameter of 240 mm and $b/a=1.5$ was constructed. The sphere, however, failed prematurely. A close examination of the video photographs of the test indicated that the failure initiated at the interface between the liner nozzle and the composites. For this sphere of $b/a=1.5$, the thickness of

the composite was approximately 60 mm. Relating to the complex winding pattern involved in the vicinity of the liner nozzle of the sphere, the manufacturer (Courtaulds Advanced Materials, France) pointed out the difficulty in maintaining a good structural integrity of the interface between the liner nozzle and the composites for such a thickness of the sphere. The above premature failure may thus be attributed to the poor interface between the nozzle and composites. Incidentally, two IM6/epoxy spheres of $b/a=1.25$ and 1.33 of inner diameter of 240 mm were successfully tested earlier by CEA (Commissariat à l'Energie Atomique, France) where failure pressures were respectively within 10 and 4% of the predicted pressure, as shown in Figure 7. The failure pressures of these spheres, incidentally, were much less than our present design objective. One possible way of increasing the failure pressure keeping the same b/a ratio is to consider the design of hybrid spheres. Thus in view of the previous success in manufacturing sphere of $b/a=1.25$, a design restriction of limiting $b/a=1.25$ was imposed for the design of hybrid spheres.

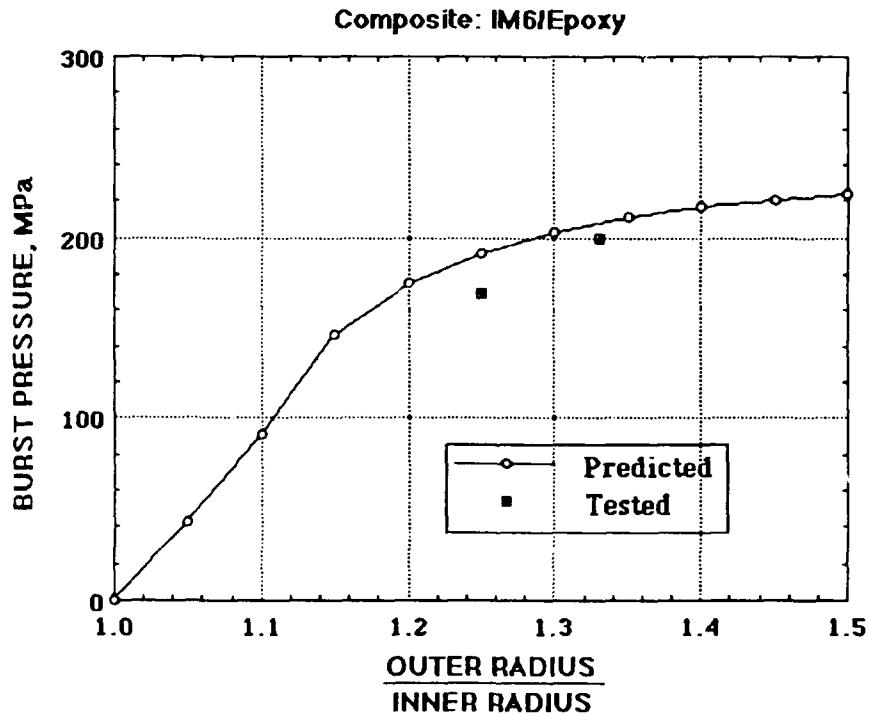


Figure 7. Comparison of the predicted burst pressure with the tested data. Material: IM6/Epoxy

The stress and strength analysis discussed above is applied for the design of two-layered hybrid spheres made of T300/5208 and IM6/epoxy composites. Both the layers are of quasi-isotropic laminates. The predictions of the burst pressure as functions of percent of layer thickness, m , are shown in Figure 8. The notation $[(T300)_m/(IM6)_n]$ indicates that the inner layer is made of T300/5208 composite, and thickness of the inner layer is m percent of the total thickness of the sphere. Obviously, the thickness of the outer layer is $(100-m)$ percent of the total thickness. Thus

the sum of m and n becomes 100. When either m or n becomes zero or 100, the sphere is no longer a hybrid sphere but rather a sphere of one material. It is obvious from the figure that a hybrid sphere with T300 inside and IM6 outside yields a higher burst pressure than a sphere with reversed order of the layers. It is also noticed from the figure that, for the hybrid sphere with T300 inside, if the thickness of either of the layers is varied between 20 and 80% of the total thickness, the variation of the burst pressure is limited to within only 2.5% of 240 MPa. Thus within the range of 20 to 80% of the layer thickness, any small manufacturing error in the layer thickness will hardly alter the expected burst pressure.

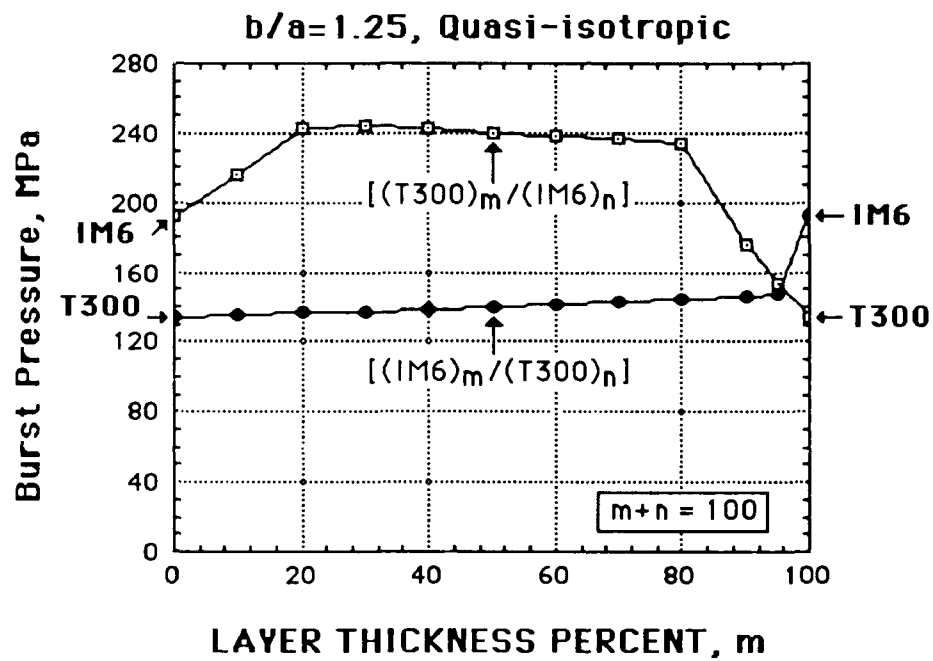


Figure 8. The burst pressure of two hybrid spheres as functions of the layer thickness.

8. Conclusions

We have presented a procedure to determine the stress, strain, and ultimate internal and external pressures of a homogenized, isotropic spherical shell of any thickness. It can be shown that the membrane solution would correspond to the tangent of the burst pressure curves in Figure 6 above.

Comparable curves for other materials will require the 3-D elastic moduli and seven strength parameters needed for the quadratic failure criterion. The collapse pressure of spherical shells under external pressure can be determined precisely the same way. Only boundary conditions need to be changed.

The required calculation can be easily programmed in a small computer. In fact, a Fortran program is written to perform the numerical analysis for multilayered (or hybrid) spheres. The instructions for executing this code are given in appendix B.

References

- (1) Lark, R.F., Filament-Wound Composite Vessel Materials Technology, Second International Conference on Pressure Vessel Technology, Part 1, Design and Analysis, ASME, Oct. 1973, pp 573-580.
- (2) Tauchert, T.R., Thermal Stresses in a Spherical Pressure Vessel Having Temperature-Dependent, Transversely Isotropic, Elastic Properties, Advances in Engineering Science, Vol. 2 (Proceedings of the 13th Annual Meeting of the Society of Engineering Science), NASA CP-2001, Nov. 1976, pp 639-651.
- (3) Bert, C.W., Analysis of Radial Filament-Reinforced Spherical Shells Under Deep Submergence Conditions, Second International Conference on Pressure Vessel Technology, Part 1, Design and Analysis, ASME, Oct. 1973, pp 529-534.
- (4) Gerstle, F.P.Jr., Analysis of Filament-Reinforced Spherical Pressure Vessels, Composite Materials: Testing and Design (Third Conference), ASTM STP 546, American Society of Testing and Materials, 1974, pp 604-631.
- (5) Gerstle, F.P.Jr., Thick-Walled Spherical Composite Pressure Vessels, appeared in Composites in Pressure Vessels and Piping, edited by S.V. Kulkarni and C.V. Zweben, ASME, PVP-PB-021, 1977, pp 69-87.
- (6) Love, A.E.H., A Treatise on the Mathematical Theory of Elasticity, Dover Publications (reprint of the fourth edition, 1927), 1944, Sections 110 and 114.
- (7) Roy, A.K. and S.W. Tsai, Three-Dimensional Effective Moduli of Orthotropic and Symmetric Laminates, to appear in the Journal of Applied Mechanics.
- (8) Tsai, S.W., Composites design, Fourth edition, Think composites, Dayton, 1988, Appendix B.

Appendix A

Method of Predicting Three-Dimensional Effective Moduli of Laminates:

The sphere is considered to be made of layers with quasi-isotropic lay-ups. The stress analysis is performed by considering the three-dimensional effective moduli of each layer. The method of predicting an equivalent homogeneous effective moduli of a laminate is discussed in detail in reference [7]. Briefly, the method is based on matching the boundary displacements of the homogeneous system with those of the laminated system of three interrelated boundary value problems (BVP). The BVP are: (a) ring subjected to equal hydrostatic pressure on both surfaces, (b) cantilever beam under end transverse load, and (c) cantilever beam subjected to uniformly distributed load on top and bottom surfaces. These interrelated BVP are selected to predict the effective moduli for in-plane and bending mode of deformation. The analyses for predicting the effective moduli are given below:

Problem 1. Ring with Hydrostatic Pressure

This problem is used to predict the interlaminar effective moduli of symmetric and orthotropic laminates for in-plane extension. For a large value of the radius to thickness ratio, r/t (r : radius, t : thickness), the deformation of the ring approximately represents the in-plane deformation. The laminated ring and its equivalent homogeneous ring are subjected to equal hydrostatic pressure on both inner and outer surface, p , as shown in Figure 9. The inner and outer displacements of the homogeneous ring are matched with those of the laminated ring to obtain effective moduli of the laminate of the ring. The interlaminar effective elastic constants obtained from this problem are \bar{E}_3^0 , v_{31}^0 , and v_{32}^0 , where v_{ij} is the Poisson's ratio for ϵ_i under σ_j . The superscript '0' is used to indicate that the elastic constants are associated with the in-plane deformation.

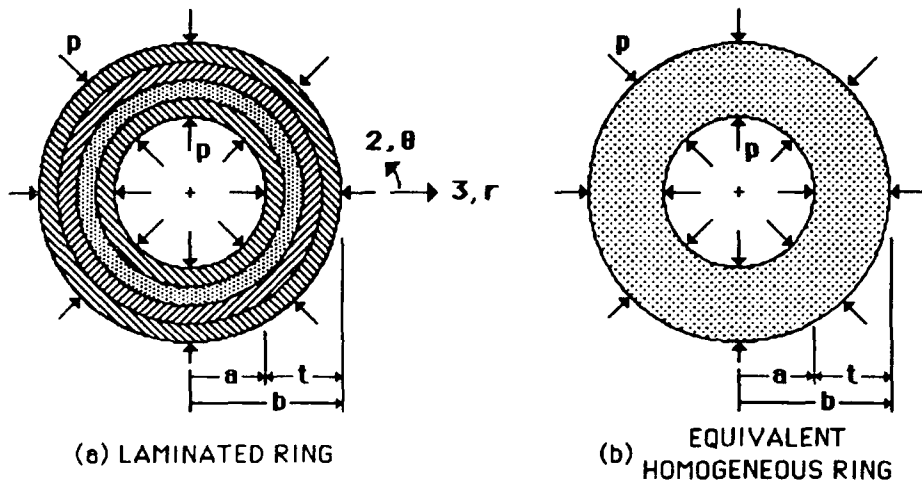


Figure 9. Configuration of the laminated and its equivalent homogeneous ring subjected to equal hydrostatic pressure on the inner and outer surface.

The method of obtaining the radial displacement of the laminated composite ring, $u^i(r)$, (Figure 9a) is given by Lekhnitskii (1968). The subscript 'i' indicates the j -th layer of the laminated ring. We do not find the necessity of repeating the procedure for obtaining the expression of $u^i(r)$ in this report. The expression for the radial displacement of the equivalent homogeneous ring (whose effective moduli are to be determined, Figure 9b) is similar to that of any layer of the laminated ring; that is:

$$u(r) = \frac{p}{1-m^{2k}} S_{23} \left\{ (m^{k+1}-1) \left(\frac{r}{b} \right)^{k-1} - (1-m^{k-1}) m^{k+1} \left(\frac{b}{r} \right)^{k+1} \right\} r \\ + \frac{p}{1-m^{2k}} S_{22} \left\{ (m^{k+1}-1) k \left(\frac{r}{b} \right)^{k-1} + (1-m^{k-1}) k m^{k+1} \left(\frac{b}{r} \right)^{k+1} \right\} r \quad (A1)$$

where $m = \frac{a}{b}$, $k = \sqrt{\frac{S_{33}}{S_{22}}}$, a : inner radius, b : outer radius, and S_{ij} ($i,j=2,3$) are the elements of the effective compliance matrix.

By equating the inner and outer displacements of the homogeneous ring with those of the laminated ring, we get two nonlinear equations in k , S_{22} , and S_{23} as follows:

$$\frac{ap}{1-m^{2k}} \left[S_{22} k (1+m^{2k}-2m^{k-1}) - S_{23} (1-m^{2k}) \right] - u^i(a) = 0, \quad (\text{for } r=a, i=1) \quad (A2)$$

$$\frac{bp}{1-m^{2k}} \left[S_{22} k (2m^{k+1}-m^{2k}-1) - S_{23} (1-m^{2k}) \right] - u^n(b) = 0, \quad (\text{for } r=b, i=n) \quad (A3)$$

The laminated ring is assumed to have n number of layers in equation (A3). Here S_{22} is considered to be known from the laminated plate theory which seems to be a reasonable assumption. Then S_{23} , k , and hence S_{33} are solved from equations (A2) and (A3) by the Newton-Raphson's technique. The laminate effective properties in terms of S_{22} , S_{23} , and S_{33} are:

$$\bar{E}_3^o = \frac{1}{S_{33}}, \quad \bar{v}_{32}^o = -\frac{S_{23}}{S_{22}} \quad (A4)$$

The constant \bar{v}_{31}^o can similarly be obtained by rotating the laminate by 90° about the r -axis of the ring (a 90° degree rotation brings the 1-axis of the laminate with the θ -direction of the ring). The superscript 'o' is, again, to denote that the effective properties apply for in-plane deformation.

Problem 2: Beam with Transverse End Load

The laminated beam is subjected to an end transverse load, P , which is modeled as an end transverse shear load. The displacement field of the laminated beam is obtained by considering the beam in the state of plane stress either in the 1-3 or in the 2-3 plane. The plane of lamination, however, is the 1-2 plane in both cases. From this problem the effective properties, \bar{G}_{13}^f , \bar{G}_{23}^f , \bar{v}_{31}^f , and \bar{v}_{32}^f are estimated. The superscript 'f' is used to indicate that the properties are associated with bending as the dominant mode of deformation.

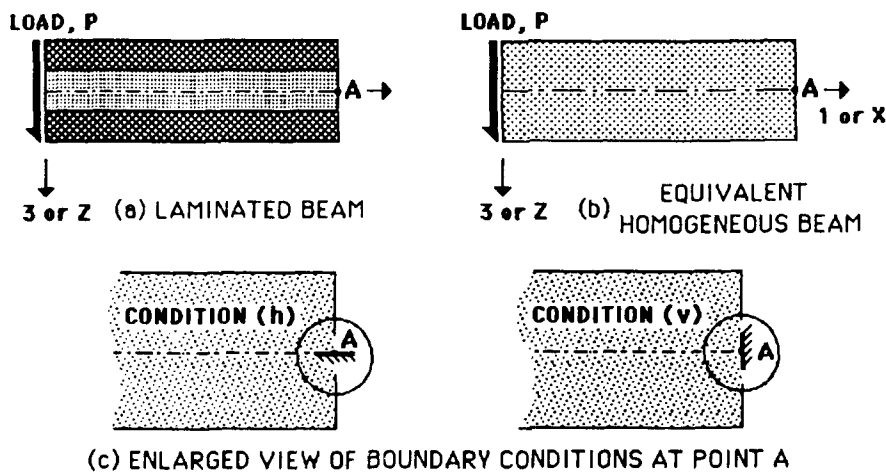


Figure 10. Configuration of the laminated beam and its equivalent homogeneous beam under end transverse load.

The expressions for the displacement field can easily be obtained by starting with an Airy stress function appropriate to this problem. Since the end transverse load, P , is modeled as the

transverse shear load, (see Figure 10), it is logical to assume that σ_z is zero everywhere in the beam. The Airy stress function, $F_j(x,z)$, for a constituent orthotropic lamina of the above problem for stresses in the (x-z or 1-3) plane, has the form

$$F_j(x,z) = A_j xz + B_j z^2 + C_j xz^2 + D_j z^3 + E_j xz^3 \quad (A5)$$

where the constants, A_j, B_j, \dots, E_j are associated with the properties of the j -th lamina. After using the linear stress-strain constitutive relations and the expressions for stresses in terms of the above stress function, $F_j(x,z)$, the displacement fields of the laminated beam, $u_j^c(x,z)$ and $w_j^c(x,z)$, along the x and z directions respectively, are:

$$u_j^c(x,z) = B_j \left[-S_{11}^{(j)} \frac{x^2}{2} + (S_{55}^{(j)} + S_{13}^{(j)}) z^2 \right] + C_j \left[-S_{11}^{(j)} x^2 z + (S_{55}^{(j)} + S_{13}^{(j)}) z^3 \right] + D_j S_{11}^{(j)} x z + E_j S_{11}^{(j)} x + Q_j z + R_j \quad (A6)$$

$$w_j^c(x,z) = A_j S_{55}^{(j)} x - B_j S_{13}^{(j)} x z + C_j \left[S_{11}^{(j)} \frac{x^3}{3} + S_{13}^{(j)} x z^2 \right] + \frac{1}{2} D_j \left[S_{13}^{(j)} z^2 - S_{11}^{(j)} x^2 \right] + E_j S_{13}^{(j)} z - Q_j x + M_j \quad (A7)$$

The constants $A_j, B_j, \dots, E_j, M_j, Q_j, R_j$, for the j -th lamina, are determined from the contact conditions at the interface of each lamina, boundary traction, P , and the boundary conditions at the support end, $x=L$. Here $S_{ij}^{(k)}$ ($i,j = 1,3,5$) are the elements of the compliance matrix of the k -th lamina.

Following a similar procedure for equations (A6) and (A7), the expressions for the displacement fields, $u^h(x,z)$ and $w^h(x,z)$, for the equivalent homogeneous beam (Figure 10b) for plane stress in (1-3) or (x-z) plane, keeping a horizontal element at point A (Figure 10) fixed, are:

$$u^h(x,z) = \frac{P}{bH^3} \left[6S_{11}(L^2 - x^2)z + 2S_{13}z^3 + S_{55}(2z^3 - \frac{3}{2}H^2z) \right] \quad (A8)$$

$$w^h(x,z) = \frac{P}{bH^3} \left[2S_{11}(x^3 - 3L^2x + 2L^3) - 6S_{13}xz^2 \right] \quad (A9)$$

where, L, b , and H are the length, width, and depth of both beams, respectively. The effective compliance matrix for the homogeneous beam, S_{ij} ($i,j=1,3,5$), is to be determined by matching the boundary displacement of the homogeneous beam with that of the laminated beam.

In Problem 1, the elements of the effective compliance matrix, S_{ij} , were predicted by matching the outer and inner displacements of the laminated and homogenized rings exactly. However in this problem the boundary displacement field of the homogeneous beam is matched with that of the laminated beam at a discrete number of boundary points by minimizing the error, Δ :

$$\Delta = \sum_{i=1}^n \left[\{ u^h(x_i, z_i) - u^c(x_i, z_i) \}^2 + \{ w^h(x_i, z_i) - w^c(x_i, z_i) \}^2 \right] \quad (A10)$$

where x_i, z_i are coordinates of the points selected along the boundary of the two beams.

After having estimated the elements of S_{ij} by minimizing Δ in equation (A10), the effective bending stiffness, and interlaminar shear stiffness and Poisson's ratio of an orthotropic and symmetric laminate for bending mode of deformation are respectively :

$$\bar{E}_1^f = \frac{1}{S_{11}}, \quad \bar{G}_{13}^f = \frac{1}{S_{55}}, \quad \bar{v}_{31}^f = -\frac{S_{13}}{S_{11}} \quad (A11)$$

The stress analysis in a similar fashion for stresses in the 2-3 plane yields the following additional effective elastic constants:

$$\bar{G}_{23}^f = \frac{1}{S_{44}}, \quad \bar{v}_{32}^f = -\frac{S_{23}}{S_{22}} \quad (A12)$$

A sensitivity study was performed on the convergence of the values of the effective properties by varying the number of points on the boundary. It was found that the bending stiffness and the interlaminar shear stiffness converged very fast with increasing numbers of points on the boundary and were practically insensitive to the ratio of the number of points chosen on the vertical lines to that of the horizontal lines of the boundary. The interlaminar Poisson's ratios were, however, somewhat sensitive to the latter ratio. We found out that the value of the ratio equal to one gave a good estimate of the Poisson's ratio, thus this value of the ratio was used in obtaining the results presented later.

Problem 3: Beam with Uniformly Distributed Load

The beam considered is under uniformly distributed load acting on the top and bottom surfaces of the beam of intensity q and p , respectively, (Figure 11). Besides all the effective properties obtained from Problem 2, one more additional property, the interlaminar effective normal stiffness, \bar{E}_3^f , is obtained from this problem. The method of predicting the effective moduli in

this problem is similar to that of Problem 3 and thus is not discussed. For details one may refer to reference [7].

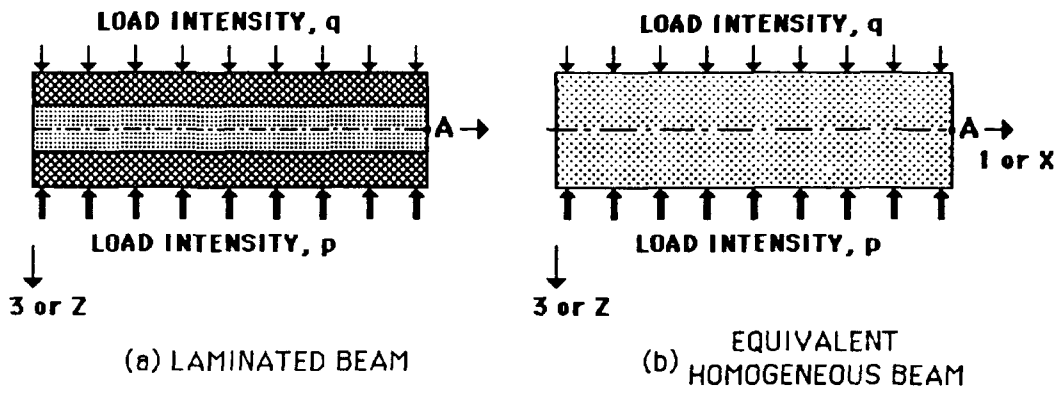


Figure 11. Configuration of the laminated beam and its equivalent homogeneous beam under uniformly distributed load on the top and bottom surface.

In general, the effective moduli of a laminate depend on the laminate stacking sequence and mode of deformation. When the laminate contains a large number of sublaminates, the effect of stacking sequence almost disappears; then the effective moduli become practically independent of mode of deformation. The values of effective moduli given below are independent of mode of deformation, thus the superscripts 'o' or 'f' are omitted from the notations below.

1) Three-dimensional properties of T300/5208 composites: [0] (unidirectional lamina)

$$\begin{array}{c}
 \begin{bmatrix} C_{xx} & C_{xy} & C_{xz} \\ C_{yy} & C_{yz} \\ C_{zz} \end{bmatrix} = \begin{bmatrix} 184.2 & 6.1 & 6.1 \\ & 14.3 & 7.5 \\ & \text{GPa} & 14.3 \end{bmatrix} \quad \begin{bmatrix} S_{xx} & S_{xy} & S_{xz} \\ S_{yy} & S_{yz} \\ S_{zz} \end{bmatrix} = \begin{bmatrix} 5.5 & -1.5 & -1.5 \\ & 97.1 & -50.5 \\ & \text{TPa}^{-1} & 97.1 \end{bmatrix} \\
 + \\
 \begin{bmatrix} C_{qq} & 0 & 0 \\ C_{rr} & 0 \\ C_{ss} \end{bmatrix} = \begin{bmatrix} 3.4 & 0. & 0. \\ & 7.2 & 0. \\ & \text{GPa} & 7.2 \end{bmatrix} \quad \begin{bmatrix} E_x & \nu_{xy} & \nu_{xz} \\ \nu_{yx} & E_y & \nu_{yz} \\ \nu_{zx} & \nu_{zy} & E_z \end{bmatrix} = \begin{bmatrix} 181. & 0.02 & 0.02 \\ 0.28 & 10.3 & 0.52 \\ 0.28 & 0.52 & 10.3 \end{bmatrix}
 \end{array}$$

$$C_{qq} = S_{qq}^{-1} = E_q, \quad C_{rr} = S_{rr}^{-1} = E_r, \quad C_{ss} = S_{ss}^{-1} = E_s$$

2) Three-dimensional effective properties of T300/5208 quasi-isotropic laminate, $[\pi/4]_s$

$$\begin{bmatrix} \bar{C}_{11} & \bar{C}_{12} & \bar{C}_{13} \\ \bar{C}_{22} & \bar{C}_{23} \\ \bar{C}_{33} \end{bmatrix} = \begin{bmatrix} 77.2 & 23.5 & 2.7 \\ & 77.2 & 2.7 \\ & & 13.0 \end{bmatrix} \text{ [GPa]} \quad \begin{bmatrix} \bar{S}_{11} & \bar{S}_{12} & \bar{S}_{13} \\ \bar{S}_{22} & \bar{S}_{23} \\ \bar{S}_{33} \end{bmatrix} = \begin{bmatrix} 14.4 & -4.3 & -2.1 \\ & 14.4 & -2.1 \\ & & 77.7 \end{bmatrix} \text{ [TPa}^{-1}\text{]}$$

$$\begin{bmatrix} \bar{C}_{44} & 0 & 0 \\ \bar{C}_{55} & 0 \\ \bar{C}_{66} \end{bmatrix} = \begin{bmatrix} 5.7 & 0. & 0. \\ & 5.7 & 0. \\ & & 26.8 \end{bmatrix} \text{ [GPa]} \quad \begin{bmatrix} \bar{E}_1 & \bar{v}_{12} & \bar{v}_{13} \\ \bar{v}_{21} & \bar{E}_2 & \bar{v}_{23} \\ \bar{v}_{31} & \bar{v}_{32} & \bar{E}_3 \end{bmatrix} = \begin{bmatrix} 69.7 & 0.30 & 0.03 \\ 0.30 & 69.7 & 0.03 \\ 0.15 & 0.15 & 12.9 \end{bmatrix}$$

$$\bar{C}_{44} = S_{44}^{-1} = \bar{G}_{23}, \bar{C}_{55} = S_{55}^{-1} = \bar{G}_{31}, \bar{C}_{66} = S_{66}^{-1} = \bar{G}_{12}$$

3) Three-dimensional properties of IM6/Epoxy composites: [0] (unidirectional lamina)

$$\begin{bmatrix} C_{xx} & C_{xy} & C_{xz} \\ C_{yy} & C_{yz} \\ C_{zz} \end{bmatrix} = \begin{bmatrix} 208.9 & 9.2 & 9.2 \\ & 17.9 & 10.9 \\ & & 17.9 \end{bmatrix} \text{ [GPa]} \quad \begin{bmatrix} S_{xx} & S_{xy} & S_{xz} \\ S_{yy} & S_{yz} \\ S_{zz} \end{bmatrix} = \begin{bmatrix} 4.9 & -1.6 & -1.6 \\ & 89.3 & -53.6 \\ & & 89.3 \end{bmatrix} \text{ [TPa}^{-1}\text{]}$$

$$\begin{bmatrix} C_{qq} & 0 & 0 \\ C_{rr} & 0 \\ C_{ss} \end{bmatrix} = \begin{bmatrix} 3.5 & 0. & 0. \\ & 8.4 & 0. \\ & & 8.4 \end{bmatrix} \text{ [GPa]} \quad \begin{bmatrix} E_x & v_{xy} & v_{xz} \\ v_{yx} & E_y & v_{yz} \\ v_{zx} & v_{zy} & E_z \end{bmatrix} = \begin{bmatrix} 203.0 & 0.02 & 0.02 \\ 0.32 & 11.2 & 0.60 \\ 0.32 & 0.60 & 11.2 \end{bmatrix}$$

$$C_{qq} = S_{qq}^{-1} = E_q, C_{rr} = S_{rr}^{-1} = E_r, C_{ss} = S_{ss}^{-1} = E_s$$

4) Three-dimensional effective properties of IM6/Epoxy quasi-isotropic laminate, $[\pi/4]_S$

$$\begin{bmatrix} C_{11} & C_{12} & C_{13} \\ C_{22} & C_{23} \\ C_{33} \end{bmatrix} = \begin{bmatrix} 87.1 & 26.7 & 4.4 \\ & 87.1 & 4.4 \\ & \text{GPa} & 15.4 \end{bmatrix} \quad \begin{bmatrix} S_{11} & S_{12} & S_{13} \\ S_{22} & S_{23} \\ S_{33} \end{bmatrix} = \begin{bmatrix} 12.8 & -3.8 & -2.6 \\ & 12.8 & -2.6 \\ & \text{TPa}^{-1} & 66.3 \end{bmatrix}$$

$$\begin{bmatrix} C_{44} & 0 & 0 \\ C_{55} & 0 \\ C_{66} \end{bmatrix} = \begin{bmatrix} 5.0 & 0. & 0. \\ & 5.0 & 0. \\ & \text{GPa} & 30.2 \end{bmatrix} \quad \begin{bmatrix} E_1 & \nu_{12} & \nu_{13} \\ \nu_{21} & E_2 & \nu_{23} \\ \nu_{31} & \nu_{32} & E_3 \end{bmatrix} = \begin{bmatrix} 78.4 & 0.30 & 0.04 \\ 0.30 & 78.4 & 0.04 \\ 0.20 & 0.20 & 15.1 \end{bmatrix}$$

$$C_{44} = S_{44}^{-1} = G_{23}, \quad C_{55} = S_{55}^{-1} = G_{31}, \quad C_{66} = S_{66}^{-1} = G_{12}$$

5) Three-dimensional properties of E-Glass/Epoxy composites: [0] (unidirectional lamina)

$$\begin{bmatrix} C_{xx} & C_{xy} & C_{xz} \\ C_{yy} & C_{yz} \\ C_{zz} \end{bmatrix} = \begin{bmatrix} 41.6 & 5.8 & 5.8 \\ & 13.7 & 8.6 \\ & \text{GPa} & 13.7 \end{bmatrix} \quad \begin{bmatrix} S_{xx} & S_{xy} & S_{xz} \\ S_{yy} & S_{yz} \\ S_{zz} \end{bmatrix} = \begin{bmatrix} 25.9 & -6.7 & -6.7 \\ & 120.9 & -72.6 \\ & \text{TPa}^{-1} & 120.9 \end{bmatrix}$$

$$\begin{bmatrix} C_{qq} & 0 & 0 \\ C_{rr} & 0 \\ C_{ss} \end{bmatrix} = \begin{bmatrix} 2.6 & 0. & 0. \\ & 4.2 & 0. \\ & \text{GPa} & 4.2 \end{bmatrix} \quad \begin{bmatrix} E_x & \nu_{xy} & \nu_{xz} \\ \nu_{yx} & E_y & \nu_{yz} \\ \nu_{zx} & \nu_{zy} & E_z \end{bmatrix} = \begin{bmatrix} 38.6 & 0.06 & 0.06 \\ 0.26 & 8.3 & 0.60 \\ 0.26 & 0.60 & 8.3 \end{bmatrix}$$

$$C_{qq} = S_{qq}^{-1} = E_q, \quad C_{rr} = S_{rr}^{-1} = E_r, \quad C_{ss} = S_{ss}^{-1} = E_s$$

6) Three-dimensional effective properties of E-Glass/Epoxy quasi-isotropic laminate, $[\pi/4]_S$

$$\begin{bmatrix} C_{11} & C_{12} & C_{13} \\ C_{22} & C_{23} \\ C_{33} \end{bmatrix} = \begin{bmatrix} 22.3 & 7.4 & 4.8 \\ & 22.3 & 4.8 \\ & & 12.3 \end{bmatrix} \text{ GPa} \quad \begin{bmatrix} S_{11} & S_{12} & S_{13} \\ S_{22} & S_{23} \\ S_{33} \end{bmatrix} = \begin{bmatrix} 52.7 & -14.2 & -15.0 \\ & 39.9 & -15.0 \\ & & 93.3 \end{bmatrix} \text{ GPa}^{-1}$$

$$\begin{bmatrix} C_{44} & 0 & 0 \\ C_{55} & 0 \\ C_{66} \end{bmatrix} = \begin{bmatrix} 3.2 & 0. & 0. \\ & 3.2 & 0. \\ & & 7.5 \end{bmatrix} \text{ GPa} \quad \begin{bmatrix} E_1 & \nu_{12} & \nu_{13} \\ \nu_{21} & E_2 & \nu_{23} \\ \nu_{31} & \nu_{32} & E_3 \end{bmatrix} = \begin{bmatrix} 19.0 & 0.27 & 0.16 \\ 0.27 & 19.0 & 0.16 \\ 0.29 & 0.29 & 10.7 \end{bmatrix}$$

$$C_{44} = S_{44}^{-1} = G_{23}, \quad C_{55} = S_{55}^{-1} = G_{31}, \quad C_{66} = S_{66}^{-1} = G_{12}$$

Appendix B

INSTRUCTIONS FOR EXECUTING THE FORTRAN PROGRAM "sphere"

To execute the code one needs to open the application file "sphere apl", then sequentially follow the input-output sequence. The code uses a material data file "matdat.spr". This file contains the effective stiffness properties of quasi-isotropic laminates, and strength properties and Young's moduli of the unidirectional plies. The data format of the file is printed on a following page. One can easily edit the file to modify the built-in data or add new data. The method of calculating the three-dimensional effective stiffnesses is presented earlier in Appendix A. A printout of the input-output sequence of an execution run of the code is also included in this report.

```

PROGRAM SPHERE
C
C-- This procedure is to do stress and failure analyses of a thick
C-- multilayered sphere subjected to INTERNAL, EXTERNAL pressures.
C-- Each layer is assumed to be composed of quasi-isotropic lay ups,
C-- each quasi-isotropic layer is thus assumed to behave as
C-- transversely isotropic layer (isotropic plane is theta-phi
C-- plane, perpendicular to the radial direction). The code reads
C-- Material data from an existing data file named 'matdat.spr'.
C-- The material data are given in 'SI' units. The material
C-- data represent the three-dimensional effective properties of
C-- a quasi-homogeneous lay up. The format for the material data
C-- file is given below. The field length for numeric data:E9.3
C-- ****
C-- number  Name      C11  C12  C13  C22  C23
C--          C33  C44  C55  C66  X
C--          X'   Y'   Y'   S    Fxy*
C--          Fyz* alp1 alp2 bta2 Em*
C--          E1   E2   nu21 nu32 Es
C-- ****
C-- The geometric and lay-up configurations can be given interactively
C-- which should be consistent with the unit used in the data file,
C-- 'matdat.spr'. A quadratic failure criterion (TSAI-WU) is used for
C-- predicting failure loads. The procedure is limited to
C-- analyzing rings (pressure vessels) of maximum 25 layers.

```

```

C-- developed by
C-- ****
C-- *   AJIT K. ROY      *
C-- *   UDRI             *
C-- *   300 College Park *
C-- *   DAYTON, OH 45469-0001 *
C-- *   (513) 255-9104   *
C-- ****

```

```

REAL   KM
CHARACTER*9 DF1
CHARACTER*1 TAB
DIMENSION SM11(25),SM12(25),SM13(25),SM33(25),KM(25),CM(25)
DIMENSION QUE(26),SGR(25,11),SGT(25,11),EU(25,11),CT11(25)
DIMENSION CT12(25),CT13(25),CT33(25),AR(25,11),PROP(10,25)
DIMENSION STRR(25,11),STRT(25,11)
DIMENSION AM(26),YY(25,11),INDX(25)

```

```

C   EXTERNAL F,FPRIM

```

```

COMMON /CLK/ SM11,SM12,SM13,SM33,KM,CM,AM
COMMON /STRNTH/ CT11,CT12,CT13,CT33,PROP
COMMON /SSDP/ SGR,SGT,STRR,STRT,EU,YY,AR

```

```

C-- the subroutine 'PLYLUP' is for sphere geometry, material
C-- property input, and calculations for layer stiffness and
C-- compliance.

```

```

CALL PLYLUP(INDX,QUE,NM,DF)

```

```

C-- the subroutine 'CALQUS' is for the calculation of the

```

```

C      interlayer tractions 'q'
      CALL  CALQUS (NM,QUE)

C--  the subroutine 'STSDSP' is for the computation of the
C      stresses, strains, and radial displacement
      CALL  STSDSP (NM,QUE,ND)

      WRITE(*,*) 'INPUT OUTPUT FILE NAME (max 9 char)'
      READ(*,'(A)') DF1
      OPEN(7,FILE=DF1,STATUS='UNKNOWN')
      WRITE(*,*) '*** PLEASE WAIT ***'

      TAB = CHAR(9)
C
      WRITE(7,*) 'inner radius(meter), outer radius(meter)'
      WRITE(7,*) AM(1),TAB,AM(NM+1)
      WRITE(7,*) 'b/a SPHERE'
      BOA = AM(NM+1)/AM(1)
      WRITE(7,*) BOA
      WRITE(7,*) 'mat #    r,meter      sig(r),MPa      sig(th)=sig(phi),
+MPa'
      WRITE(7,340) ((INDX(I),TAB,YY(I,J),TAB,
+ SGR(I,J)/1.E6,TAB,SGT(I,J)/1.E6,J=1,ND),I=1,NM)
      WRITE(7,*) 'mat #    r,meter      eps(r)      eps(th)=eps(phi)
+u(r),mm'
      WRITE(7,345) ((INDX(I),TAB,YY(I,J),TAB,
+ STRR(I,J),TAB,STRT(I,J),TAB,EU(I,J)*1000,J=1,ND),I=1,NM)
C
C
      CALL  STRIO (NM,ND,ITK,JTK,ARMN,DF,INDX)
C

      WRITE(7,*) 'mat #    r(meter)    strength ratio'
      WRITE(7,342) ((INDX(I),TAB,YY(I,J),TAB,AR(I,J),J=1,ND),I=1,NM)
      WRITE(7,*) 'FAILURE LOCATION & FAILURE PRESSURE'
      WRITE(7,*) 'mat #    r(meter), INT PRESSURE, EXT PRESSURE (in Pa)'
      WRITE(7,345) INDX(ITK),TAB,YY(ITK,JTK),TAB,AR(ITK,JTK)*QUE(1),
+ TAB,AR(ITK,JTK)*QUE(NM+1)
      WRITE(7,360)

360  FORMAT('END OF OUTPUT')
340  FORMAT(2X,I2,A1,E12.6,A1,E12.6,A1,E12.6)
342  FORMAT(2X,I2,A1,E12.6,A1,E12.6)
345  FORMAT(2X,I2,A1,E12.6,A1,E12.6,A1,E12.6,A1,E12.6)
      CLOSE(7,STATUS='KEEP')
      STOP
      END
C
C
*****SUBROUTINE PLYLUP(INDX,QUE,NM,DF)
*****SUBROUTINE PLYLUP(INDX,QUE,NM,DF)

C--  This subroutine is to obtain the geometric and lay-up

```

```
c-- configuration of the ring. The Ply Degradation Factor (DF)
c-- is also given interactively for the prediction of Last-Ply-Fail
c-- -ure or Burst Pressure.
c
c      CHARACTER TYP*21, WISH*7
c      REAL NPLY,KM
c      DIMENSION PROP(10,25),AM(26),PLYPRP(25),SM11(25),SM12(25)
c      DIMENSION SM13(25),SM33(25),KM(25),CM(25)
c      DIMENSION CT11(25),CT12(25),CT13(25),CT33(25)
c      DIMENSION INDX(25),NPLY(25),QUE(26)
c
c      COMMON /CLK/ SM11,SM12,SM13,SM33,KM,CM,AM
c      COMMON /STRNTH/ CT11,CT12,CT13,CT33,PROP
c
c
c      WRITE(*,21)
21      FORMAT(/, 'INPUT INNER DIAMETER',/, '?')
      READ(*,*) DMTINR
c      DMTINR=2.0
c      LNTH=1.0
c
c      WRITE(*,*) 'INPUT THE VALUE OF b/a OF THE SPHERE'
      READ(*,*) BOAS
c
c      WRITE(*,22)
22      FORMAT('INPUT INTERNAL PRESSURE & EXTERNAL PRESSURE',/, '?')
      READ(*,*) QUE1,QUEN
c      QUE1=1.0
c      QUEN=1.0
c
c
c      OPEN(8,FILE='matdat.spr',STATUS='OLD')
c
c      WRITE(*,10)
10      FORMAT(/,T25,'*****MATERIAL INFORMATION*****')
      WRITE(*,11)
11      FORMAT(/,T15,'INDEX NUMBER      MATERIAL DESCRIPTION',
+           /,T15, '-----')
c
c      I = 0
1      CONTINUE
c      I = I+1
      READ(8,20,END=2) IND,TYP, (PROP(I,J),J=1,25)
20      FORMAT(2X,I2,A21,T27,5E9.3,/,T27,5E9.3,/,T27,5E9.3,
+           /,T27,5E9.3)
c
c      WRITE(*,12) IND,TYP
12      FORMAT(T23,I2,T30,A23)
      GOTO 1
c
c      I = I-1
2      CLOSE(UNIT=8, STATUS='KEEP')
c
c      ITR = 0
c      WRITE(*,*) 'input MATERIAL NUMBER for the mandrel'
```

```

C      READ(*,*) INDX(1)
C      WRITE(*,*) '*** INPUT PLY LAYUP INFORMATION (max 25 layers)***'
C51    IR=IR+1
C      WRITE(*,*) 
C
C      WRITE(*,*) 'INPUT THE VALUE OF THE DEGRADATION FACTOR'
C      WRITE(*,*) ' for INTACT plies: DF=1'
C      READ(*,*) DF
C      DF=1.0
C      BOAS= 1.+1./AOTS

C      mandrel displacement
C      AM(1) = 0.5*DMTINR
C      AM(2) = BOAM*AM(1)
C      NPLY(1) = AM(2) - AM(1)

      WRITE(*,*) 'INPUT NO OF LAYERS (max 25 layers)'
      READ(*,*) NM

      DO 25 I=1,NM+1
      QUE(I) = 0.0
25    CONTINUE

      QUE(1) = QUE1
      QUE(NM+1) = QUEN

      DO 51 IR=1,NM

      WRITE(*,*) '*** LAYERS ARE NUMBERED FROM INSIDE TO OUTSIDE ***'
      WRITE(*,*) 
      WRITE(*,*) '*** FOR LAYER ',IR,' ***'
      WRITE(*,*) 'INPUT MATL INDEX NO. & THICKNESS FACTOR'
C
      READ(*,*) INDX(IR),NPLY(IR)
      NPLY(IR)=NPLY(IR)*(BOAS-1.)*AM(1)
51    CONTINUE

      DO 53 IR=1,NM

      DO 50 I = 1,25
      PLYPRP(I) = PROP(INDX(IR),I)
50    CONTINUE
C
C-- degradation of effective stiffness and compressive strength

      PLYPRP(2) = DF* PLYPRP(2)
      PLYPRP(3) = DF*PLYPRP(3)
      PLYPRP(5) = DF* PLYPRP(5)
C

      AM(IR+1) = AM(IR) + NPLY(IR)
      CM(IR) = AM(IR)/AM(IR+1)
C
      CALL BTCLCT(PLYPRP,IR)

```

```
C      KM(IR) = 0.5*SQRT(1.+8.* (CT11(IR)+CT12(IR)-CT13(IR))/CT33(IR))
C      WRITE(*,*) 'DO YOU WANT TO ADD ANOTHER PLY LAYUP? (Y OR N)'
C      READ(*,'(A)') WISH
C
53    CONTINUE
C      IF(WISH .EQ. 'Y') GOTO 51
C
C      RETURN
C      END
C
C      ****
C      SUBROUTINE BTCLCT(PLYPRP,ITR)
C--      this subroutine is to perform some intermediate calculations
C--      required for the routine 'CALQUS'.
C
C      REAL   KM
C
C      DIMENSION PLYPRP(25),SMTX(6,6),CT11(25),CT12(25),CT13(25)
C      DIMENSION CT33(25),AM(26),CTX(6,6),PROP(10,25)
C      DIMENSION XX(6,1),KM(25),CM(25)
C      DIMENSION SM11(25),SM12(25),SM13(25),SM33(25)
C
C      COMMON /CLK/ SM11,SM12,SM13,SM33,KM,CM,AM
C      COMMON /STRNTH/ CT11,CT12,CT13,CT33,PROP
C
C      DO 10 I = 1,6
C          XX(I,1) = 0.0
C      DO 11 J = 1,6
C          CTX(I,J) = 0.0
C          SMTX(I,J) = 0.0
11    CONTINUE
10    CONTINUE
C
C
C      CTX(1,1) = PLYPRP(1)
C      CTX(1,2) = PLYPRP(2)
C      CTX(1,3) = PLYPRP(3)
C      CTX(2,1) = CTX(1,2)
C      CTX(2,2) = PLYPRP(4)
C      CTX(2,3) = PLYPRP(5)
C      CTX(3,1) = CTX(1,3)
C      CTX(3,2) = CTX(2,3)
C      CTX(3,3) = PLYPRP(6)
C      CTX(4,4) = PLYPRP(7)
C      CTX(5,5) = PLYPRP(8)
C      CTX(6,6) = PLYPRP(9)
C
C
C      DO 15 I=1,6
C      DO 16 J=1,6
C          SMTX(I,J) = CTX(I,J)
16    CONTINUE
```

```

15    CONTINUE

    CALL GAUSSJ(SMTX, 6, 6, XX, 1, 1)

C
C
    CT11(ITR) = CTX(1,1)
    CT12(ITR) = CTX(1,2)
    CT13(ITR) = CTX(1,3)
    CT33(ITR) = CTX(3,3)

C
    SM11(ITR) = SMTX(1,1)
    SM12(ITR) = SMTX(1,2)
    SM13(ITR) = SMTX(1,3)
    SM33(ITR) = SMTX(3,3)

C
    RETURN
    END

C ****
C SUBROUTINE CALQUS(NM,QUE)

C-- this subroutine is to calculate the inter-layer normal pressure
C-- Q's from a set of simultaneous equations.

    REAL KM,MUE
    REAL AA,BB
    DIMENSION SM11(25),SM12(25),SM13(25),SM33(25),CM(25)
    DIMENSION AA(25,25),QUE(26),ALF(25),BTM(25),BB(25,1)
    DIMENSION SGR(25,11),SGT(25,11),STRR(25,11),PROP(10,25)
    DIMENSION STRT(25,11),EU(25,11),YY(25,11),AR(25,11)
    DIMENSION CT11(25),CT12(25),CT13(25),CT33(25)
    DIMENSION AM(26),KM(25),MUE(25),GMA(25)

    COMMON /CLK/ SM11,SM12,SM13,SM33,KM,CM,AM
    COMMON /STRNTH/ CT11,CT12,CT13,CT33,PROP
    COMMON /SIZE/ AA,BB
    COMMON /SSDP/ SGR,SGT,STRR,STRT,EU,YY,AR

    DO 10 I = 1, NM-1

        BB(I,1) = 0.0

        DO 11 J = 1,NM-1
            AA(I,J) = 0.0
11        CONTINUE
10        CONTINUE

        DO 20 I=1,NM

            MUE(I) = (1.-CM(I)**(2.*KM(I)))*((KM(I)+.5)*CT33(I)
1                -2.*CT13(I))*((KM(I)-.5)*CT33(I)+2.*CT13(I))
            ALF(I) = 2.*KM(I)*CT33(I)*CM(I)**(KM(I)+.5)/MUE(I)

            BTM(I) = (1.-CM(I)**(2.*KM(I)))*(5*CT33(I)-2.*CT13(I))

```

```
1           /MUE(I)
GMA(I) = KM(I)*(1.+CM(I)**(2.*KM(I)))*CT33(I)/MUE(I)

20    CONTINUE

    IF (NM .EQ. 1) GOTO 50

    IF ((NM-1) .EQ. 1) THEN

        AA(1,1) = (BTM(2)-BTM(1)-GMA(2)-GMA(1))*AM(2)
        BB(1,1) = -QUE(NM+1)*AM(3)*ALF(2)/CM(2)-QUE(1)*AM(1)*ALF(1)
        QUE(2) = BB(1)/AA(1,1)
        ELSE
        DO 40 I=1,NM-1

        IF (I .EQ. 1) THEN

            BB(I,1) = -AM(I)*ALF(I)*QUE(1)
            AA(I,I) = AM(2)*(BTM(I+1)-BTM(I)-GMA(I+1)-GMA(I))
            AA(I,I+1) = AM(3)*ALF(I+1)/CM(I+1)

        ELSEIF (I .EQ. (NM-1), THEN

            BB(I,1) = -AM(I+1)*ALF(I+1)*QUE(NM+1)/CM(I+1)
            AA(I,NM-1) = AM(I+1)*(BTM(I+1)-BTM(I)-GMA(I+1)-GMA(I))
            AA(I,NM-2) = AM(I)*ALF(I)

        ELSE
            BB(I,1) = 0.0
            AA(I,I-1) = AM(I)*ALF(I)
            AA(I,I) = AM(I+1)*(BTM(I+1)-BTM(I)-GMA(I+1)-GMA(I))
            AA(I,I+1) = AM(I+2)*ALF(I+1)/CM(I+1)

        ENDIF

40    CONTINUE

    NMM1 = NM-1
    IFAIL = 0

    CALL GAUSSJ(AA,NMM1,25,BB,1,1)

    DO 30 I=1, NM-1
    QUE(I+1) = BB(I,1)
30    CONTINUE

    ENDIF

50    CONTINUE

    RETURN
    END
C ****
SUBROUTINE STSDSP(NM,QUE,ND)
```

c-- to calculate stress, strain and displacement field based on
c-- the thick sphere formulation.

REAL KM

DIMENSION YY(25,11),SGR(25,11),SGT(25,11),EU(25,11),SM11(25)
DIMENSION SM12(25),SM13(25),SM33(25),CM(25),AM(26),KM(25)
DIMENSION CT11(25),CT12(25),CT13(25),CT33(25),PROP(10,25)
DIMENSION AR(25,11),STRR(25,11),STRT(25,11)
DIMENSION QUE(26)

COMMON /CLK/ SM11,SM12,SM13,SM33,KM,CM,AM
COMMON /STRNTH/ CT11,CT12,CT13,CT33,PROP
COMMON /SSDP/ SGR,SGT,STRR,STRT,EU,YY,AR

WRITE(*,*)
WRITE(*,*) 'INPUT NO OF EQUIDISTANT CALCULATION POINTS THRU'
+THICKNESS IN EACH LAYER'
WRITE(*,*) '(max 11, min 2)'
READ(*,*) ND

DO 40 I =1,NM

FCT = (AM(I+1)-AM(I))/(ND-1)
CNST1 = 1./(1.-CM(I)**(2.*KM(I)))
CNST2 = (KM(I)-.5)*CT33(I) + 2.*CT13(I)
CNST3 = (KM(I)+.5)*CT33(I) - 2.*CT13(I)
CNST4 = CT11(I)+CT12(I)+(KM(I)-.5)*CT13(I)
CNST5 = CT11(I)+CT12(I)-(KM(I)+.5)*CT13(I)

DO 45 J = 1,ND
YY(I,J) = AM(I) + (J-1)*FCT

c-- I : for layers, increasing from inside to outside
c-- J : for calculation points, increasing from inside to outside

c-- radial stress
SGR(I,J) = CNST1*((QUE(I)*CM(I)**(KM(I)+1.5)-QUE(I+1))*
1 (YY(I,J)/AM(I+1))**(KM(I)-1.5) -
2 (QUE(I)-QUE(I+1)*CM(I)**(KM(I)-1.5))*
3 CM(I)**(KM(I)+1.5)*(AM(I+1)/YY(I,J))**(KM(I)+1.5))
c-- hoop stress
SGT(I,J) = CNST1*(CNST4/CNST2)*(QUE(I)*CM(I)**(KM(I)+1.5)
1 -QUE(I+1))*(YY(I,J)/AM(I+1))**(KM(I)-1.5) +
2 CNST1*(CNST5/CNST3)*(QUE(I)-QUE(I+1)*
3 CM(I)**(KM(I)-1.5))*
4 CM(I)**(KM(I)+1.5)*(AM(I+1)/YY(I,J))**(KM(I)+1.5)

45 CONTINUE
40 CONTINUE

DO 50 I=1,NM
DO 60 J=1,ND

```
c-- radial strain
    STRR(I,J) = SM33(I)*SGR(I,J)+2.*SM13(I)*SGT(I,J)

c-- hoop strain
    STRT(I,J) = SM13(I)*SGR(I,J)+(SM11(I)+SM12(I))*SGT(I,J)

c-- radial displacement
    EU(I,J) = STRT(I,J)*YY(I,J)

60    CONTINUE
50    CONTINUE

    RETURN
    END

C ****
C SUBROUTINE STRIO(NM,ND,ITK,JTK,ARMN,DF,INDX)

c-- to obtain the strength ratio for predicting the failure
c-- pressure.

DIMENSION SM11(25),SM12(25),SM13(25),SM33(25),KM(25)
DIMENSION CM(25),AM(25),INDX(25),PROP(10,25),CMTX(6,6)
DIMENSION CT11(25),CT12(25),CT13(25),CT33(25)
DIMENSION SGR(25,11),SGT(25,11),STRR(25,11),STRT(25,11)
DIMENSION EU(25,11),YY(25,11),AR(25,11),PLYPRP(25)
DIMENSION GE(6,6),GEE(6),AF(6,6),AFF(6)

COMMON /CLK/ SM11,SM12,SM13,SM33,KM,CM,AM
COMMON /STRNTH/ CT11,CT12,CT13,CT33,PROP
COMMON /SSDP/ SGR,SGT,STRR,STRT,EU,YY,AR

DO 2 I=1,6
      AFF(I) = 0.0
DO 3 J=1,6
      AF(I,J) = 0.0
3    CONTINUE
2    CONTINUE

DO 10 I=1,NM

DO 50 IR = 1,25
    PLYPRP(IR) = PROP(INDX(I),IR)
50    CONTINUE

c-- degradation of unidirectional stiffness properties

    PLYPRP(11) = DF**0.2*PLYPRP(11)
    PLYPRP(22) = DF* PLYPRP(22)
    PLYPRP(23) = DF*PLYPRP(23)
    PLYPRP(25) = DF* PLYPRP(25)

c-- 3: fiber direction
```

```

c-- 1 & 2: transverse to the fiber
AF(1,1) = 1./(PLYPRP(12)*PLYPRP(13))
AF(2,2) = AF(1,1)
AF(3,3) = 1./(PLYPRP(10)*PLYPRP(11))
AF(4,4) = 1./(PLYPRP(14)**2)
AF(5,5) = AF(4,4)
AF(6,6) = 0.60/PLYPRP(10)
AFF(1) = 1./PLYPRP(12) - 1./PLYPRP(13)
AFF(2) = AFF(1)
AFF(3) = 1./PLYPRP(10) - 1./PLYPRP(11)
AF(1,2) = PLYPRP(16)*SQRT(AF(1,1)*AF(2,2))
AF(1,3) = PLYPRP(15)*SQRT(AF(1,1)*AF(3,3))
AF(2,3) = AF(1,3)
AF(2,1) = AF(1,2)
AF(3,1) = AF(1,3)
AF(3,2) = AF(2,3)

CALL CTX3D(PLYPRP,CMTX)

CALL G3DCLT(CMTX,AF,AFF,GE,GEE)

DO 11 J=1,ND

AA = ABS((GE(3,3)+2.*GE(3,2)+GE(2,2))*STRT(I,J)**2
1      +2.*GE(3,1)+GE(2,1))*STRT(I,J)*STRR(I,J)
2      +GE(1,1)*STRR(I,J)**2)

BB = (GEE(3)+GEE(2))*STRT(I,J)+GEE(1)*STRR(I,J)

c-- strength ratios based on thick preeuse vessel solution
AR(I,J) = -(BB/(2.*AA)) +SQRT((BB/(2.*AA))**2 +1./AA)

11  CONTINUE
10  CONTINUE

c-- ARMN: minimum value of strength ratios based on thick pressure
c-- vessel solution.

CALL VARMN(AR,ARMN,NM,ND,ITK,JTK)

RETURN
END

C ****
SUBROUTINE VARMN(AR,ARMN,NM,ND,ITK,JTK)

DIMENSION AR(25,11)

ITK = 1
JTK = 1
ARMN = AR(1,1)

```

```

DO 12 I=1,NM
DO 11 J = 1,ND

IF(AR(I,J) .GE. ARMN) GOTO 11
ITK = I
JTK = J
ARMN = AR(I,J)
11  CONTINUE
12  CONTINUE

RETURN
END
C ****
SUBROUTINE G3DCLT(CTX,AF,AFF,GE,GEE)

DIMENSION CTX(6,6),GE(6,6),TMP1(6,6),GEE(6),TMP2(6)
DIMENSION AF(6,6), AFF(6)

DO 5 I=1,6
DO 7 J=1,6
TMP2(I) = 0.0
TMP1(I,J) = 0.0
GE(I,J) = 0.0
7  CONTINUE
5  CONTINUE

DO 10 I=1,6
DO 11 J=1,6
DO 12 K=1,6
TMP1(I,J) = TMP1(I,J) + AF(I,K)*CTX(K,J)
12  CONTINUE
11  CONTINUE
10  CONTINUE

DO 20 I=1,6
DO 21 J=1,6
DO 22 K=1,6
GE(I,J) = GE(I,J) + CTX(I,K)*TMP1(K,J)
22  CONTINUE
21  CONTINUE
20  CONTINUE

DO 30 I=1,6
DO 31 J=1,6
TMP2(I) = TMP2(I) + AFF(J)*CTX(J,I)
31  CONTINUE
30  CONTINUE

DO 40 I=1,6
GEE(I) = TMP2(I)
40  CONTINUE

RETURN
END

C-- ****
C-- the routine for solving a system of simultaneous equations

```

```

SUBROUTINE GAUSSJ(A,N,NP,B,M,MP)
PARAMETER (NMAX=50)
DIMENSION A(NP,NP),B(NP,MP),IPIV(NMAX),INDXR(NMAX),INDXC(NMAX)
DO 11 J=1,N
  IPIV(J)=0
11  CONTINUE
DO 22 I=1,N
  BIG=0.
  DO 13 J=1,N
    IF (IPIV(J).NE.1) THEN
      DO 12 K=1,N
        IF (IPIV(K).EQ.0) THEN
          IF (ABS(A(J,K)).GE.BIG) THEN
            BIG=ABS(A(J,K))
            IROW=J
            ICOL=K
          ENDIF
          ELSE IF (IPIV(K).GT.1) THEN
            PAUSE 'Singular matrix'
          ENDIF
        ENDIF
     12  CONTINUE
      ENDIF
   13  CONTINUE
    IPIV(ICOL)=IPIV(ICOL)+1
    IF (IROW.NE.ICOL) THEN
      DO 14 L=1,N
        DUM=A(IROW,L)
        A(IROW,L)=A(ICOL,L)
        A(ICOL,L)=DUM
   14  CONTINUE
      DO 15 L=1,M
        DUM=B(IROW,L)
        B(IROW,L)=B(ICOL,L)
        B(ICOL,L)=DUM
   15  CONTINUE
    ENDIF
    INDXR(I)=IROW
    INDXC(I)=ICOL
    IF (A(ICOL,ICOL).EQ.0.) PAUSE 'Singular matrix.'
    PIVINV=1./A(ICOL,ICOL)
    A(ICOL,ICOL)=1.
    DO 16 L=1,N
      A(ICOL,L)=A(ICOL,L)*PIVINV
   16  CONTINUE
    DO 17 L=1,M
      B(ICOL,L)=B(ICOL,L)*PIVINV
   17  CONTINUE
    DO 21 LL=1,N
      IF (LL.NE.ICOL) THEN
        DUM=A(LL,ICOL)
        A(LL,ICOL)=0.
      DO 18 L=1,N
        A(LL,L)=A(LL,L)-A(ICOL,L)*DUM
     18  CONTINUE
      DO 19 L=1,M
        B(LL,L)=B(LL,L)-B(ICOL,L)*DUM
   19  CONTINUE

```

```
        ENDIF
21      CONTINUE
22      CONTINUE
DO 24 L=N,1,-1
      IF (INDXR(L).NE.INDXC(L)) THEN
        DO 23 K=1,N
          DUM=A(K,INDXR(L))
          A(K,INDXR(L))=A(K,INDXC(L))
          A(K,INDXC(L))=DUM
23      CONTINUE
      ENDIF
24      CONTINUE
      RETURN
      END

C-- ****
C-- SUBROUTINE CTX3D(PLYPRP,CTX)
C-- formulation of three-dimensional PLY stiffness matrix

      REAL NU21
      DIMENSION PLYPRP(25),CTX(6,6)

      NU21 = PLYPRP(23)*PLYPRP(22)/PLYPRP(21)
      VE = 1./( (1.+PLYPRP(24))* (1.-PLYPRP(24)-2.*PLYPRP(23)*NU21))
C
      CTX(1,1) = (1.-NU21*PLYPRP(23))*VE*PLYPRP(22)
      CTX(1,2) = (PLYPRP(24)+NU21*PLYPRP(23))*VE*PLYPRP(22)
      CTX(1,3) = NU21*(1.+PLYPRP(24))*VE*PLYPRP(21)
      CTX(2,1) = CTX(1,2)
      CTX(2,2) = CTX(1,1)
      CTX(2,3) = CTX(1,3)
      CTX(3,1) = CTX(1,3)
      CTX(3,2) = CTX(2,3)
      CTX(3,3) = (1.-PLYPRP(24)**2)*VE*PLYPRP(21)
      CTX(4,4) = PLYPRP(25)
      CTX(5,5) = CTX(4,4)
      CTX(6,6) = (1.-PLYPRP(24)-2.*NU21*PLYPRP(23))*VE*PLYPRP(22)/2.

      RETURN
      END
```

Listing of the material data file "matdat.spr" for SPHERE

1	T3/5203[pi/4]	.772E11	.235E11	.27E10	.772E11	.27E10
		.13E11	.57E10	.57E10	.268E11	.15E10
		.15E10	.40E8	.246E9	.68E8	-0.5E0
		-.80E0	.02E-6	22.5E-6	.6E-6	0.20
		.181E12	.103E11	.28E0	0.52E0	.717E10
2	H-IM6/EP[pi/4]	.871E11	.267E11	.44E10	.871E11	.44E10
		.154E11	.50E10	.50E10	.302E11	.35E10
		.154E10	.56E8	.15E9	.98E8	-0.50E0
		-.80E0	.0	0.0	0.0	0.1
		.203E12	.112E11	0.32E0	0.60E0	.84E10
3	E-Glass[pi/4]	.223E11	.737E10	.477E10	.223E11	.477E10
		.123E11	.319E10	.319E10	.747E10	.106E10
		.61E9	.31E8	.118E9	.72E8	-0.5E0
		-.80E0	8.6E-6	22.1E-6	0.6E-6	0.07
		.386E11	.827E10	0.26E0	0.60E0	.414E10
4	AL 2014	.101E12	.462E11	.462E11	.101E12	.462E11
		.101E12	.276E11	.276E11	.276E11	.449E9
		.897E9	.449E9	.897E9	.283E9	-0.5E0
		-0.5E0	23.2E-6	23.2E-6	0.0	0.0
		.725E11	.725E11	0.313E0	0.313E0	.276E11
5	SS AM350	.284E12	.133E12	.133E12	.284E12	.133E12
		.284E12	.75E11	.75E11	.75E11	.114E10
		.228E10	.114E10	.228E10	.738E9	-0.5E0
		-0.5E0	11.7E-6	11.7E-6	0.0	0.0
		.200E12	.200E12	0.318E0	0.318E0	.750E11

Number	Name	C11	C12	C13	C22	C23
		C33	C44	C55	C66	X
		X'	Y	Y'	S	Fxy*
		Fyz*	alf1	alf2	bta2	Em*
		Ex	Ey	nu21	nu32	Es

Cij's are the elements of the effective stiffness matrix in Pa
 Ei's are the elements of the Young's Moduli of an unidirectional ply in Pa

This is the print out of the input-output sequence for the code "sphere". This run is for a hybrid sphere of $b/a=1.25$, and 50% of thickness of T300/5208 inside and rest of IM6/Epoxy outside. The sphere is subjected to internal pressure.

INPUT OUTPUT FILE NAME
T3IM6

INPUT INNER DIAMETER
?
>1.0

INPUT THE VALUE OF b/a OF THE SPHERE
>1.25

INPUT INTERNAL PRESSURE & EXTERNAL PRESSURE
?
>1 0

*****MATERIAL INFORMATION*****

INDEX NUMBER	MATERIAL DESCRIPTION
1	T3/5203[pi/4]
2	H-IM6/E ^P [pi/4]
3	E-Glass[pi/4]
4	AL 2014
5	SS AM350

*** INPUT PLY LAYUP INFORMATION (max 25 layers)***

INPUT NO OF LAYERS (max 25 layers)
>2

** LAYERS ARE NUMBERED FROM INSIDE TO OUTSIDE **

*** FOR LAYER 1 ***
INPUT MATL INDEX NO. & THICKNESS FACTOR
>1 .5

** LAYERS ARE NUMBERED FROM INSIDE TO OUTSIDE **

*** FOR LAYER 2 ***
INPUT MATL INDEX NO. & THICKNESS FACTOR
>2 .5

INPUT NO OF EQUIDISTANT CALCULATION POINTS THRU THICKNESS IN EACH LAYER
(max 11, min 2)
>3

*** PLEASE WAIT ***

LISTING OF THE OUTPUT FILE "T3IM6"

```
inner radius(meter), outer radius(meter)
.500000 .625000
b/a SPHERE
1.25000
mat # r,meter    sig(r),MPa    sig(th)=sig(phi),MPa
1 0.500000E+00  -.100000E-05  0.244346E-05
1 0.531250E+00  -.637914E-06  0.194125E-05
1 0.562500E+00  -.377960E-06  0.162349E-05
2 0.562500E+00  -.377959E-06  0.179410E-05
2 0.593750E+00  -.166265E-06  0.159966E-05
2 0.625000E+00  0.000000E+00  0.149123E-05
mat # r,meter    eps(r)      eps(th)=eps(phi)    u(r),mm
1 0.500000E+00  -.879822E-10  0.266238E-10  0.133119E-07
1 0.531250E+00  -.577207E-10  0.208252E-10  0.110634E-07
1 0.562500E+00  -.361736E-10  0.170920E-10  0.961423E-08
2 0.562500E+00  -.343097E-10  0.170920E-10  0.961423E-08
2 0.593750E+00  -.192543E-10  0.148012E-10  0.878822E-08
2 0.625000E+00  -.765717E-11  0.134000E-10  0.837503E-08
mat # r(meter)  strength ratio
1 0.500000E+00  0.240422E+09
1 0.531250E+00  0.307092E+09
1 0.562500E+00  0.348892E+09
2 0.562500E+00  0.327183E+09
2 0.593750E+00  0.368268E+09
2 0.625000E+00  0.272434E+09
FAILURE LOCATION & FAILURE PRESSURE
mat # r(meter), INT PRESSURE, EXT PRESSURE (in Pa)
1 0.500000E+00  0.240422E+09  0.000000E+00
END OF OUTPUT
```